Saito, I., Kawabata, H., Fujiwara, T., Sugiyama, H., & Matsuura, T. (1989) *J. Am. Chem. Soc. 111*, 8302–8303.
Shepodd, T. J., Petti, M. A., & Dougherty, D. A. (1988) *J. Am. Chem. Soc. 110*, 1983–1985.
Sekine, T., Kato, K. A., Takamori, K., Machida, M., & Kanaoka, Y. (1974) *Biochim. Biophys. Acta 354*, 139–147.
Snyder, J. P. (1989) *J. Am. Chem. Soc. 111*, 7630–7632.
Sugiura, Y., Shiraki, T., Konishi, M., & Oki, T. (1990) *Proc. Natl. Acad. Sci. U.S.A. 87*, 3831–3835.
Sugiyama, H., Xu, C., Murugesan, N., Hecht, S. M., van der Marel, G. A., & van Boom, J. H. (1988) *Biochemistry 27*, 58–67.
Szajewski, R. P., & Whitesides, G. M. (1980) *J. Am. Chem. Soc. 102*, 2011–2026.
Whitesides, G. M., Lilburn, J. E., & Szajewski, R. P. (1977) *J. Org. Chem. 42*, 332–338.
Wilson, J. M., Bayer, R. J., & Hupe, D. J. (1977) *J. Am. Chem. Soc. 99*, 7922–7926.
Zein, N., Sinha, A. M., McGahren, W. J., & Ellestad, G. A. (1988) *Science 240*, 1198–1201.
Zein, N., Ding, W.-D., & Ellestad, G. A. (1990) in *Molecular Basis of Specificity in Nucleic Acid–Drug Interactions* (Pullman, B., & Jortner, J., Eds.) pp 323–330, Kluwer Academic Publishers, New York.

Neocarzinostatin-Mediated DNA Damage in a Model AGT·ACT Site: Mechanistic Studies of Thiol-Sensitive Partitioning of C4′ DNA Damage Products†

Peter C. Dedon,‡ Zhi-Wei Jiang, and Irving H. Goldberg*
Department of Biological Chemistry and Molecular Pharmacology, Harvard Medical School, Boston, Massachusetts 02115
Received October 30, 1991; Revised Manuscript Received December 19, 1991

ABSTRACT: Double-strand (DS) DNA damage caused by neocarzinostatin (NCS) has been studied in the trinucleotide AGT·ACT sequence in an AP-1 transcription factor binding site. There are strong similarities between bistranded lesions produced at AGT·ACT and AGC·GCT, including the fact that DS lesions outnumber SS lesions on the AGT and AGC strands, while SS exceed DS on the ACT and GCT strands. Structure–function studies revealed that a variety of different thiols produced bistranded lesions in this model by predominantly C4′-hydrogen atom abstraction (84–93%) at the T of AGT and C5′-hydrogen atom abstraction (87–91%) at the T of ACT. Single-strand (SS) lesions were found to represent a variable mixture of C4′ and C5′ chemistry. The C4′-hydroxylated abasic site occurred in both SS and DS lesions at both sites and accounted for most of the DS damage at AGT (60–83%); the remaining damage consisted of 3′-phosphoglycolate- and 3′-phosphate-ended fragments. The nature of the thiol was found to affect the partitioning of the breakdown products arising from C4′ and, to a lesser extent, C5′ hydrogen atom abstraction. Production of 3′-phosphoglycolate residues, restricted mainly to the T of AGT in bistranded lesions, correlated with the incidence of direct DS breaks in the AGT·ACT model and in plasmid DNA and appeared to be influenced by the reducing power of the thiol activator. Furthermore, hydrazine and sodium borohydride both inhibited the formation of glycolate, an effect that was exploited to determine the rate constant for 3′-phosphoglycolate formation: 0.06 min^{-1} at 0 °C, pH 7.4. Under anaerobic conditions, the nitroaromatic radiation sensitizer misonidazole caused a large increase in glycolate production in both SS and DS lesions formed by NCS, which suggests that the formation of 3′-phosphoglycolate, like 3′-formylphosphate generated by C5′ chemistry, involves an oxyradical intermediate. The pathways for DNA damage involving C4′ and C5′ hydrogen atom abstraction thus share many common features, several of which are consistent with a mechanism for the production of NCS-mediated bistranded lesions at AGT·ACT that involves a tetraoxide bridge joining the lesions on opposite strands of DNA.

The enediyne core of the antibiotic antitumor agent neocarzinostatin (NCS)[1] binds to DNA via the minor groove and, following nucleophilic attack by a thiol, rearranges to form a bicyclic diradical species that abstracts hydrogen atoms from the deoxyribose sugar of DNA [see Scheme I in the accompanying paper (Dedon & Goldberg, 1992); for review, see Goldberg (1991)]. The carbon-centered radicals add molecular oxygen to form peroxyradicals, which undergo degradation to unique sugar fragments depending on the location of the abstracted hydrogen (Scheme I of this paper). At the C4′-position, breakdown of the peroxyradical partitions to form a 4′-hydroxylated abasic site (Saito et al., 1989; Frank et al., 1991; Kappen et al., 1991) or to produce a strand break with a 3′-phosphoglycolate residue and a 5′-phosphate (Frank et al., 1991; Kappen et al., 1991). Similarly, the strand break resulting from the degradation of the C5′-peroxyradical involves either a nucleoside 5′-aldehyde at the 5′-end and a 3′-phosphate (Kappen et al., 1982; Kappen & Goldberg, 1983) or a labile 3′-formylphosphate-ended DNA fragment and a 5′-phosphate (Kappen & Goldberg, 1984; Chin et al., 1987) (Scheme I). Abstraction of the C1′-hydrogen atom, the third

† This work was supported by Grants CA44257 and GM12573 from the N.I.H. (I.H.G.) and by a Bristol-Myers Squibb Fellowship (P.C.D.).
* Author to whom correspondence should be addressed.
‡ Present address: Division of Toxicology, Massachusetts Institute of Technology, Cambridge, MA 02139.

[1] Abbreviations: NCS, neocarzinostatin chromophore; GSH, glutathione; MPA, 3-mercaptopropionate; TG, thioglycolate; CYS, cysteine; MMPA, methyl 3-mercaptopropionate; CSM, cysteamine; E-CYS, ethyl cysteine; MTG, methyl thioglycolate; BME, 2-mercaptoethanol; DTT, dithiothreitol; HTP, 4-hydroxythiophenol; SS, single strand; DS, double strand; AP, apurinic/apyrimidinic; bp, base pair.

0006-2960/92/0431-1917$03.00/0

Scheme I: Proposed Mechanism of NCS-Induced DNA Damage at C1′, C4′, and C5′

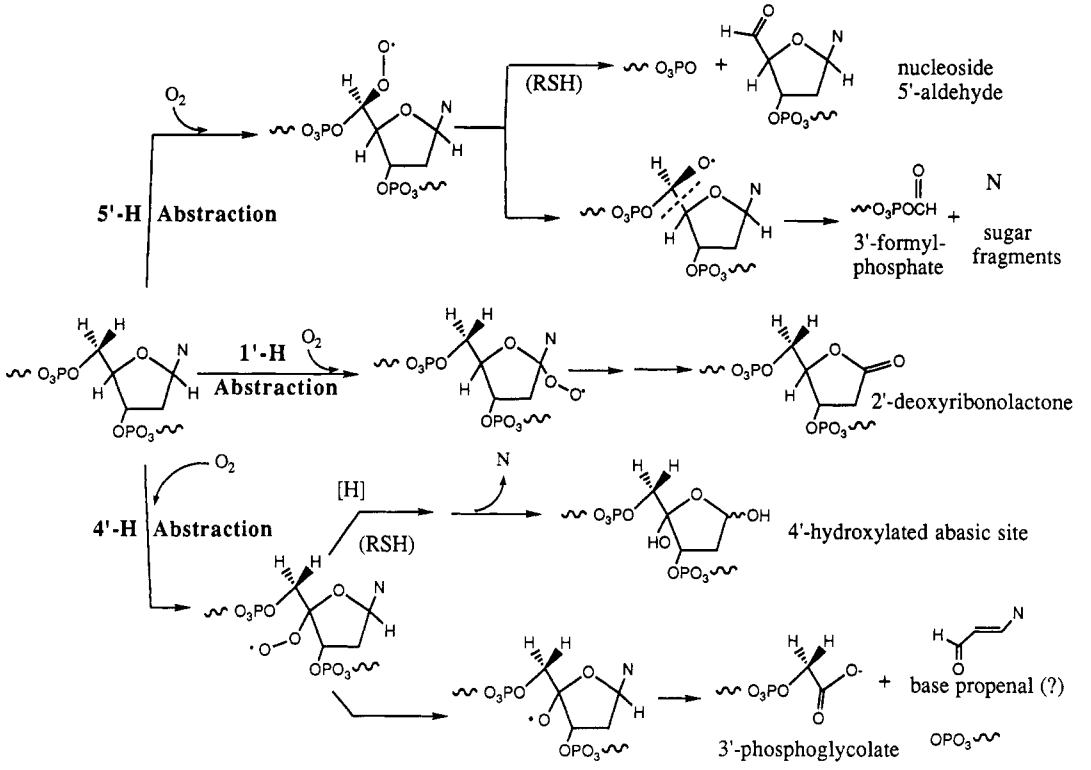

hydrogen atom accessible from the minor groove, and formation of the peroxyradical results in the production of an alkali-labile 2′-deoxyribonolactone abasic site (Kappen & Goldberg, 1989).

Single-strand (SS) breaks, the predominant lesions produced by NCS, arise mainly by C5′ hydrogen atom abstraction at T and A residues. While there is a base preference for these lesions (Kappen & Goldberg, 1983), there is no clear-cut sequence specificity for SS breaks (Takeshita et al., 1981; Lee & Goldberg, 1989). Double-strand (DS) breaks have in the past been attributed to the random coincidence of nonspecific SS breaks at closely opposed sites on opposite strands (Poon et al., 1977; Hatayama & Goldberg, 1979; Beerman et al., 1983), a conclusion based on the high ratios of SS to DS breaks produced by thiols such as 2-mercaptoethanol (BME) (Poon et al., 1977; Boye et al., 1984). However, more recent evidence with other thiols indicates that bistranded lesions produced by NCS all have a trinucleotide sequence specificity and appear to result from the action of a single molecule of NCS (Povirk et al., 1988; Dedon & Goldberg, 1990).

The presence of a thiol molecule as a covalent adduct of the DNA-damaging diradical form of NCS suggests that the thiol could have a significant influence on the type of damage produced by NCS. Recent studies suggest that the thiol influences both the selection of the hydrogen atom abstracted by NCS and the partitioning of the sugar breakdown products (Frank et al., 1991; Kappen et al., 1991). Further, the nature of the thiol appears to influence the relative quantities of SS and DS breaks (Dedon & Goldberg, 1990). We have undertaken a series of structure–function studies with several different thiols to clarify the role of the thiol in NCS activity. In the preceding paper, the nature of the thiol was found to affect the rate of activation of NCS and the relative quantities of NCS-mediated SS and DS breaks in plasmid DNA (Dedon & Goldberg, 1992). The present work examines the biochemistry of lesions produced by NCS at a model site for bistranded lesions, the AP-1 transcription factor binding site

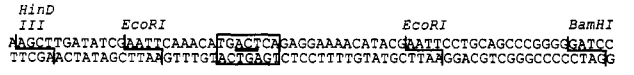

FIGURE 1: AP-1 site sequence. The *Eco*RI fragment containing a heptanucleotide AP-1 binding site (boxed sequence) was subcloned into pBluescript as described in Materials and Methods. The AGT·ACT site for NCS-mediated bistranded lesions is underlined. The *Hin*dIII and *Bam*HI restriction sites employed for end-labeling are noted at each end of the sequence.

(Figure 1). At the center of this site lies the trinucleotide sequence most frequently involved in direct DS breaks produced by NCS: AGT·ACT (Dedon & Goldberg, 1990). Bistranded lesions at this site occur mainly by abstraction of the C4′-hydrogen atom at the T of AGT and the C5′-hydrogen atom at the T of ACT. The 2-bp, 3′-stagger of the cleavage sites, along with strand break analysis in plasmids, suggests that the DS breaks are caused by a single drug molecule (Dedon & Goldberg, 1990, 1992).

The studies presented here address three different aspects of NCS-mediated damage at the AGT·ACT model site. First, the model site has allowed the chemical characterization of the NCS-mediated damage at all four ends of the bistranded lesion, in both SS and DS breaks at AGT·ACT. The DNA damage produced by several different thiol activators was then compared to gain insight into the role of the thiol in NCS activity, particularly the partitioning of the sugar breakdown products. Finally, the mechanism of the formation of 3′-phosphoglycolate was examined with the aid of the radiation sensitizer misonidazole. These results will be discussed in light of the findings on the mechanism of activation of NCS by thiols reported in the accompanying paper (Dedon & Goldberg, 1992).

Materials and Methods

Materials. Neocarzinostatin chromophore was prepared and stored as described elsewhere (Dedon & Goldberg, 1992). The AP-1 binding site construct, FSE2-pUC19, was kindly

provided by Michael Greenberg and Victor Rivera, Department of Microbiology and Molecular Genetics, Harvard Medical School. pBluescript was obtained from Promega.

Preparation of the AP-1 Site Model. The 31-bp *Eco*RI fragment from FSE2-pUC19, which contains the AP-1 binding site, was subcloned into the *Eco*RI site of pBluescript KS$^+$ according to standard procedures (Ausubel et al., 1989). The orientation of the new construct (pAP1-3; Figure 1) was verified by Maxam–Gilbert sequencing of the 61-bp *Hin*dIII/*Bam*HI fragment with 5′-[^{32}P] end-labeling at the *Hin*dIII site (Maxam & Gilbert, 1980). [^{32}P] End-labeling at the *Hin*dIII and *Bam*III sites was performed by standard methods (Ausubel et al., 1989) and was followed by cleavage with *Pvu*II to yield the following fragments: *Hin*dIII/*Pvu*II, 221 bp, and *Bam*HI/*Pvu*II, 325 bp.

Drug/DNA Reactions. DNA cleavage was initiated by adding NCS to a final concentration of 1 μM to a solution of end-labeled DNA (5×10^4 to 1×10^5 cpm), 30 μg/mL calf thymus DNA, 6 mM EDTA, 50 mM HEPES, pH 7.4, and thiol, added as either an aqueous (GSH, TG, MPA, CYS, CSM, E-CYS, BME, and DTT) or a methanolic (MMPA, MTG, and HTP) solution. For the *Hin*dIII/*Pvu*II fragment, 50 mM NaCl was included in the reaction mixture to prevent denaturation of the DS cleavage fragment. The reaction was allowed to proceed for 1.5 h at 0 °C. For 5′-[^{32}P] end-labeled fragments, hydrazine (1 M, pH 8) was then added to 100 mM to form the pyridizine derivative of the 4′-hydroxylation product, and the reaction was allowed to occur at room temperature for 1 h, followed by ethanol precipitation with 0.3 M sodium acetate, pH 5.2. Occasionally, hydrazine treatment occurred after ethanol precipitation and resuspension in water; no differences were noted for either order of hydrazine treatment and precipitation. In the glycolate-formation kinetics experiments, hydrazine was added at various times following addition of NCS, and the reaction was allowed to proceed for 1 h at room temperature, followed by ethanol precipitation. Nucleoside 5′-aldehyde residues generated in drug-treated, 3′-[^{32}P] end-labeled fragments were reduced with sodium borohydride as described previously (Kappen & Goldberg, 1983), following addition of HEPES (1 M, pH 7) to 100 mM final concentration.

Experiments in which NCS treatment occurred under anaerobic conditions in the presence of misonidazole were performed as described previously (Kappen & Goldberg, 1985). The 5′-[^{32}P]-labeled *Bam*HI/*Pvu*II fragment was treated with 1 μM NCS in the presence of 30 μg/mL calf thymus DNA and 5 mM GSH under these conditions.

Gel Analysis of Cleavage Products. Nondenaturing polyacrylamide gels (12%, 30:1 acrylamide:bisacrylamide, 0.8 mm, 30 × 40 cm) in TBE buffer (Tris–borate–EDTA; Ausubel et al., 1989) were employed to resolve DNA fragments produced by DS cleavage. Drug-treated DNA was resuspended in 5 μL of loading buffer, consisting of 20 mM HEPES, pH 7, 2 mM EDTA, 50 mM NaCl, 5% glycerol, and bromophenol blue, at 0 °C. The samples were loaded onto the gel and run at 4 °C for 7000 V·h (approximately 3500 V·h for gels analyzed on the Betascope).

Gels were then processed as follows. Analysis of hydrazine-sensitive DS breaks in nondenaturing gels was accomplished by fixing the gels in 10% methanol/10% acetic acid for several minutes, drying the gel, and quantitating radioactivity in the entire lane (total) and the AGT·ACT DS break fragment with a Model 603 Betascope (Betagen). For analysis of SS and DS lesions on sequencing gels, the bands corresponding to the SS breaks (band remaining at origin of

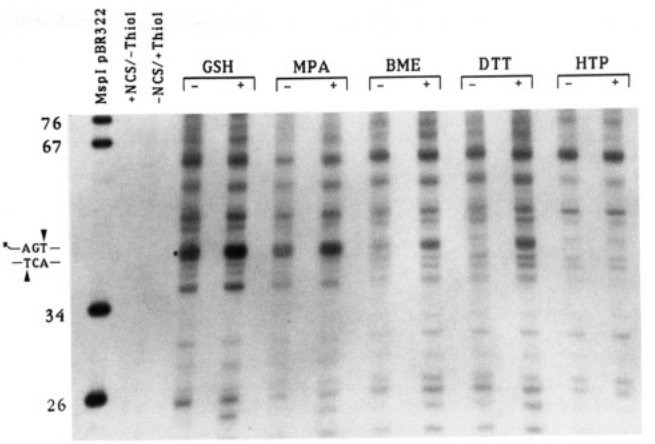

FIGURE 2: Double-stranded breaks produced by NCS. The 5′-[^{32}P]-labeled *Bam*HI/*Pvu*II fragment was treated with NCS in the presence of five different thiols and either derivatized with hydrazine (+) or left untreated (−). The duplex DNA then was resolved on a 12% nondenaturing polyacrylamide gel. The numbers in the left margin represent the sizes (bp) of the 5′-[^{32}P]-labeled *Msp*I-digested pBR322 size standards (first lane). Controls without added thiol or drug are shown in the second and third lanes, respectively. The asterisk denotes the position of the double-strand break at AGT·ACT, which is illustrated in the left margin.

nondenaturing gel) and the DS break at AGT·ACT were excised by alignment of an autoradiogram, and the DNA was isolated by the crush and soak method (Ausubel et al., 1989). The DNA in each band was resolved on a 20% polyacrylamide sequencing gel (20:1 acrylamide:bisacrylamide, 0.4 mm, 60 × 30 cm; Owl Scientific) for the 5′-[^{32}P] end-labeled fragments or on a 10% polyacrylamide sequencing gel (0.4 mm, 40 × 30 cm; BRL) for the 3′-[^{32}P] end-labeled fragments (Maxam & Gilbert, 1980). The gels were usually dried following fixation in 10% methanol/10% acetic acid, and the band location was determined in autoradiograms (Kodak XOmat AR film) relative to Maxam–Gilbert sequencing standards (Maxam & Gilbert, 1980). Bands were quantitated by densitometry (LKB Ultrascan XL laser densitometer) of lightly exposed, preflashed films (Laskey & Mills, 1975).

Results

Biochemistry of the AGT·ACT Lesions in the AP-1 Site. The AP-1 binding site (Figure 1) was employed as a model to study the damage produced by NCS at the T's of the AGT·ACT sequence. To identify the cleavage sites and the chemistry of the damage, SS and DS breaks in NCS-treated DNA were resolved in nondenaturing gels (Figure 2) and the excised bands of DNA were subjected to sequencing gel resolution (Figures 3 and 4). The DNA fragments generated by NCS have unique sugar residues attached to either their 3′- or 5′-ends (Scheme I), which alter the migration of the fragments in sequencing gels relative to phosphate-ended fragments generated by Maxam–Gilbert chemical sequencing reactions (Maxam & Gilbert, 1980). This altered mobility is presumptive evidence for the identity of the attached residue and, subsequently, the hydrogen atom abstracted by NCS. All of the damaged sugar residues identified in this work have been previously subjected to chemical characterization (Maxam & Gilbert, 1980; Kappen et al., 1982, 1991; Kappen & Goldberg, 1983; Saito et al., 1989; Frank et al., 1991).

Table I represents a quantitative summary of the damage at AGT and ACT in the AP-1 site derived from gels like those shown in Figures 3 and 4. Scheme II shows all of the cleavage products known to occur with NCS-mediated DNA damage at the T of either AGT or ACT and serves as a key for the

Table I: Summary of NCS-Mediated DNA Damage at AGT-ACT with Several Thiol Activators[a]

		double-strand breaks					single-strand breaks				
		3′-end			5′-end		3′-end			5′-end	
thiol	site	3′-P[b]	3′-G[c]	H[c]	5′-P[d]	5′-A[b]	3′-P[b]	3′-G[c]	H[c]	5′-P[d]	5′-A[b]
GSH	AGT	11	23	66	100	0	51	0	49	44	56
	ACT	91	1	8	26	74	75	1	24	14	86
MPA	AGT	7	29	64	100	0	67	0	33	56	44
	ACT	89	0	11	29	71	56	2	42	29	71
BME	AGT	16	24	60	100	0	54	0	46	34	66
	ACT	87	0	13	10	90	47	0	53	20	80
DTT	AGT	16	1	83	100	0	63	0	37	41	59
	ACT	91	0	9	10	90	66	0	34	19	81
HTP	AGT	*e*	*e*	*e*	*e*	*e*	59	0	41	9	91
	ACT	*e*	*e*	*e*	*e*	*e*	74	0	26	5	95

[a] Scheme II summarizes lesions produced at T of either AGT or ACT. Abbreviations for chemical species at damaged T residue appear in both Scheme II and Table I: 3′-P, 3′-phosphate; 3′-G, 3′-phosphoglycolate; H, 4′-hydroxylated abasic site; 5′-P, 5′-phosphate; 5′-A, nucleoside 5′-aldehyde. Residues are grouped according to their attachment to either the 3′- or 5′-ends. Relative quantities of lesions (percent of total damage) at either 3′- or 5′-ends are given in the table; 4′-hydroxylation product was measured as 3′-phosphopyridizine derivative, so it is included in the percentage of 3′-end residues; averages of 2–3 experiments. [b] 5′ deoxyribose hydrogen atom was abstracted to produce this lesion (see also Scheme I). [c] 4′ deoxyribose hydrogen atom was abstracted to produce this lesion (see also Scheme I). [d] 4′ or 5′ deoxyribose hydrogen atom was abstracted to produce this lesion (see also Scheme I). [e] No DS breaks detected.

Scheme II: Summary of NCS-Mediated DNA Damage at the T of AGT and ACT[a]

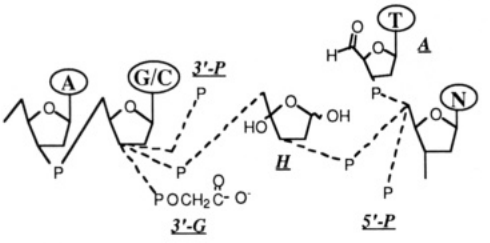

[a] See Table I for key to abbreviations.

damage quantitated in Table I. The mechanisms of formation of the cleavage products are shown in Scheme I, and the hydrogen atom abstracted to produce them is indicated in the footnote to Table I and in Scheme I. Table I itself contains the relative quantities of these various sugar residues attached to either the 3′- or 5′-ends of the DNA fragments produced by cleavage at T; since the 4′-hydroxylated abasic site was detected as the 3′-phosphopyridizine derivative, it is included in the relative quantities of 3′-residues. The relative contributions of C4′ and C5′ chemistry to the damage at the AGT and ACT sites can be determined from the relative quantities of 3′-end groups: 3′-phosphate, arising from the breakdown of 3′-formylphosphate residues and from cleavage to produce the nucleoside 5′-aldehyde (C5′ chemistry) (Scheme I), and 3′-phosphoglycolate and 3′-phosphopyridizine, arising from C4′ hydrogen atom abstraction (Scheme I).

To illustrate the Table I entries, consider the DS damage produced when GSH is the activator. At the T of AGT in the 5′-[^{32}P]-labeled *Bam*HI/*Pvu*II fragment, 66% of the damage was found to be the 3′-phosphopyridizine derivative of the 4′-hydroxylated abasic site (band a in Figure 3A), 23% of the damage involved 3′-phosphoglycolate-ended fragments (band c in Figure 3A), and 11% had 3′-phosphate ends (band b in Figure 3A). This indicates that 89% (55% + 23%) of the DS DNA damage at the T of AGT was caused by C4′ hydrogen atom abstraction and 11% by C5′ hydrogen atom abstraction. The 3′-phosphate-ended fragments at the T of AGT presumably arise from the formylphosphate pathway only, since nucleoside 5′-aldehyde was not detectable at the other side of the AGT cleavage in the 3′-[^{32}P]-labeled *Hin*dIII/*Pvu*II fragment (see Figure 3B). In SS breaks, more than half of the cleavage at AGT results in 5′-nucleoside aldehyde (asterisk in Figure 3B; Table I), which suggests a SS bias in the formation of nucleoside 5′-aldehyde residues. On the ACT strand, 91% of the damage at the T of ACT arises from C5′ hydrogen atom abstraction, as indicated by the predominance of 3′-phosphate-ended fragments (asterisk in Figure 4B).

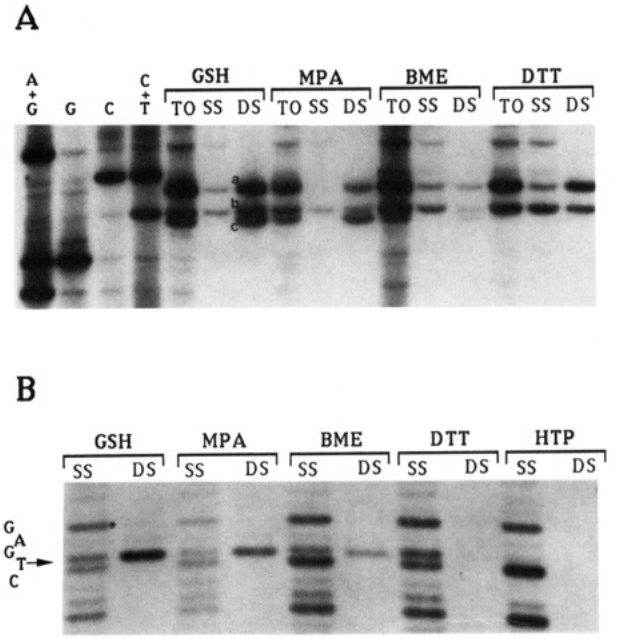

FIGURE 3: Sequencing gel analysis of NCS-mediated damage at AGT and identification of DNA damage involving the T of AGT at either the 5′- or 3′-end of the cleavage site. (Panel A) The 5′-[^{32}P]-labeled *Bam*HI/*Pvu*II fragment was treated with NCS in the presence of different thiols, the hydrazine-treated DNA was resolved on a 12% nondenaturing gel, and the isolated DS break fragment at the AGT-ACT was resolved on a 60-cm 20% sequencing gel. The letters labeling the first four lanes are Maxam–Gilbert chemical sequencing standards. The three lanes for each thiol represent total damage in unfractionated DNA (TO), SS-nicked DNA (SS; DNA remaining at the origin of the nondenaturing gel), and the DS break fragment (DS). The letters to the left of the GSH DS bands denote the migrations of different damaged forms: (a) 3′-pyridizine derivative of the 4′-hydroxylated abasic site, (b) 3′-phosphate-ended DNA, and (c) 3′-phosphoglycolate-ended DNA. (Panel B) The 3′-[^{32}P]-labeled *Hin*dIII/*Pvu*II fragment was treated as noted above except that the DNA was treated with sodium borohydride to stabilize nucleoside 5′-aldehyde residues (asterisk). The eluted DS break DNA was resolved on a 40-cm 10% sequencing gel. The letters in the left margin denote the DNA sequence; the arrow indicates the position of the phosphate-ended fragment generated by the Maxam–Gilbert C+T reaction. The notations SS and DS are as described for panel A.

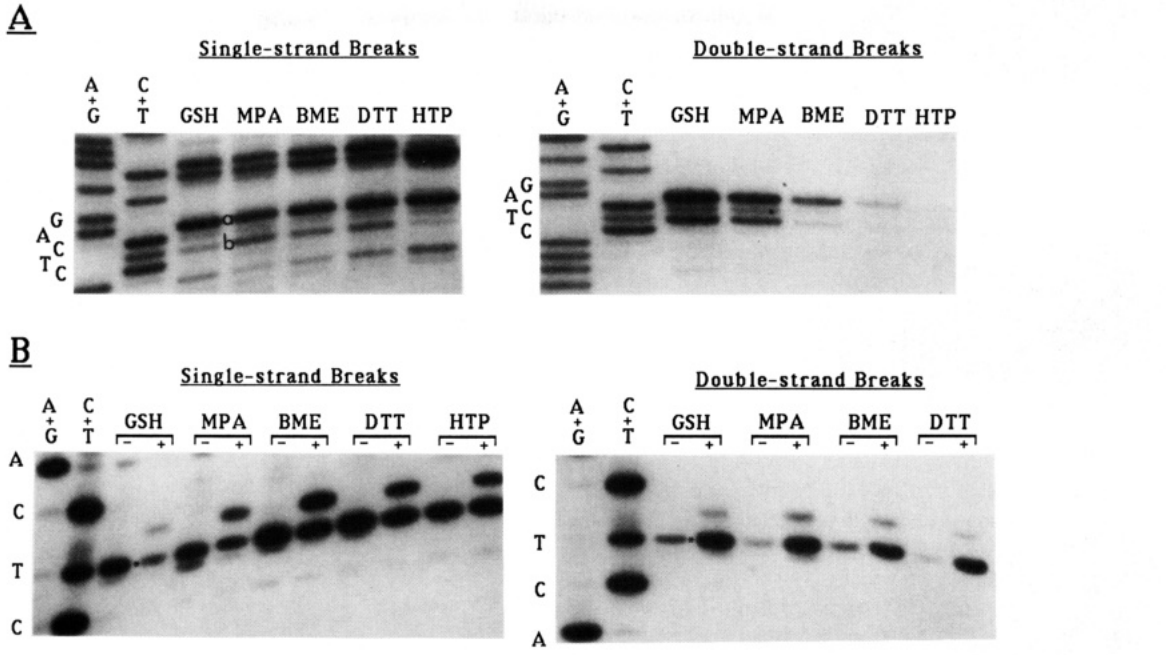

FIGURE 4: Sequencing gel analysis of the NCS-induced damage at ACT and identification of the damage at the T of ACT at either the 3′- or 5′-end of the cleavage site. (Panel A) The 3′-[^{32}P]-labeled *Bam*HI/*Pvu*II fragment was treated as in panel B of Figure 3 and the DNA was resolved on a 40-cm 10% sequencing gel (SS breaks on left, DS breaks on right). The first two lanes are Maxam–Gilbert chemical sequencing standards, and letters in the left margin denote the sequence. DNA fragments are denoted as follows: (a) the 5′-nucleoside aldehyde-ended fragment; (b) the 5′-phosphate-ended fragment. (Panel B) The 5′-[^{32}P]-labeled *Hin*dIII/*Pvu*II fragment was treated as noted in panel A of Figure 3 and the DNA was resolved on a 60-cm 20% sequencing gel. The first two lanes and the letters along the left margin denote the sequence. The two columns under each thiol represent control (−) and hydrazine-treated (+) samples. The asterisk denotes the position of the 3′-phosphate-ended fragment. The weak signal for the hydrazine-sensitive SS breaks with GSH is due to poor recovery of the DNA in this sample.

In the original observation of direct DS breaks at AGT·ACT (Dedon & Goldberg, 1990), the presence of abasic sites produced by NCS was not addressed. These lesions consist of either the 4′-hydroxylation product arising from abstraction of the C4′ hydrogen atom (Saito et al., 1989; Frank et al., 1991; Kappen et al., 1991) or the 2′-deoxyribonolactone produced when the C1′ hydrogen atom is removed (Kappen & Goldberg, 1989; Kappen et al., 1990). The strand remains intact at these sites, so that DNA with a bistranded lesion involving an abasic site with a closely opposed break on the other strand would be present as full-length duplex restriction fragment on the nondenaturing gel. Hydrazine converts the 4′-hydroxylated abasic site to a strand break with 3′-phosphopyridizine and 5′-phosphate ends (Sugiyama et al., 1988). With GSH as activator, hydrazine derivatization of the NCS-treated AP-1 site reveals the presence of 4′-hydroxylated abasic sites in DS and SS breaks on both strands (Figure 3A and 4B; Table I). This abasic site represents nearly 70% of the total damage at AGT in bistranded lesions produced by NCS and GSH and 90% of the small amount of C4′ damage at ACT (Table I). Treatment with putrescine, an agent that cleaves both types of abasic site (Povirk et al., 1988), does not reveal significantly more damage at AGT beyond that revealed by hydrazine, which suggests that there are few if any 2′-deoxyribonolactone abasic sites and thus little C1′ chemistry at AGT (data not shown). The previous conclusion of predominantly C4′ chemistry at the T of AGT and C5′ chemistry at the T of ACT (Dedon & Goldberg, 1990) strands correct in spite of the revelation of the 4′-hydroxylated abasic sites in bistranded lesions.

At the T of ACT, the small quantity of C4′ hydrogen atom abstraction that occurs in bistranded lesions consists almost entirely of 4′-hydroxylated abasic site with little, if any, glycolate (Figure 4B). Nucleoside 5′-aldehyde is the predominant product from the C5′-hydrogen atom abstraction in both SS and DS breaks (band a in Figure 4A; Table I). It must be kept in mind that stabilization of the aldehyde by reduction with sodium borohydride also stabilizes the 4′-hydroxylated abasic site against cleavage (Rabow et al., 1986), so that residues at ACT associated with an abasic site on the other strand would not be apparent in these experiments. However, in NCS/GSH-treated DNA samples that were exposed to hydrazine prior to reduction of the aldehyde, the ratio of aldehyde to phosphate is similar to the situation with reduction alone, with allowance made for some degradation of the nucleoside 5′-aldehyde during the 1-h hydrazine treatment at room temperature (data not shown).

Effect of Different Thiols on NCS-Mediated Damage at AGT·ACT. Previous studies have suggested that the nature of the thiol not only affects the relative quantity of SS and DS breaks produced by NCS (Dedon & Goldberg, 1990, 1992) but also may affect the partitioning that occurs between the two pathways for degradation of the deoxyribose sugar following removal of the C4′ or C5′ hydrogen atoms (Kappen et al., 1991). Eight different thiols were examined for their effects on the damage produced by NCS at the model AGT·ACT site. Figure 2 shows an example of the nondenaturing gel resolution of DS breaks in the 5′-[^{32}P]-labeled *Bam*HI/*Pvu*II fragment produced when NCS is activated by several different thiols. DNA fragments generated by DS breaks at AGT·ACT migrate as double bands on the nondenaturing gels (asterisk in Figure 2), with the top band consisting mainly of fragments containing the 5′-nucleoside aldehyde and/or 3′-phosphopyridizine moieties and the bottom bands containing mainly the phosphate- and/or glycolate-ended fragments (data not shown). Plots of the relative quantities of direct and hydrazine-sensitive DS breaks produced by the various thiols in the AGT·ACT model versus those determined in plasmid DNA indicate an excellent correlation between the NCS-mediated DNA damage produced in the two model systems (slope = 0.92, r^2 = 0.96 and slope = 0.98, r^2 = 0.99 for direct and hydrazine-sensitive breaks,

respectively). The quantities (relative to GSH) of NCS-mediated direct/hydrazine-sensitive DS breaks at the AGT·ACT site are as follows: GSH, 1/1; MPA, 0.8/0.8; CYS, 0.4/1; TG, 0.2/0.4; MMPA, 0.5/0.7; CSM, 0.3/0.6; E-CYS, 0.3/0.6; MTG, 0.4/0.8; BME, 0.2/0.2; DTT, 0.1/0.3; and HTP, 0.04/0.03 (from densitometric scans of autoradiograms similar to Figure 2). The correlations with the plasmid data are not surprising since the majority of direct and hydrazine-sensitive bistranded lesions (i.e., those containing 4′-hydroxylated abasic sites) occur at GT steps, mainly at AGT·ACT and to a lesser extent at TGT·ACA (P. C. Dedon, Z.-W. Jiang, and I. H. Goldberg, unpublished observations; Dedon & Goldberg, 1990). Bistranded lesions at AGC·GCT only become apparent when the 2′-deoxyribonolactone abasic site is cleaved by putrescine (Dedon & Goldberg, 1992).

In addition to their effects on the quantities of bistranded lesions, the thiols also affect the partitioning of sugar breakdown products that occurs following removal of either the C5′ or C4′ hydrogen atoms. The data in Table I indicate that the bistranded lesions produced by all the thiols (except HTP) involve predominantly C4′ chemistry at the T of AGT and C5′ chemistry at the T of ACT, as described previously for GSH. The product distribution is also consistent between the thiols, with the 4′-hydroxylated abasic site at AGT and nucleoside 5′-aldehyde at ACT as major products in bistranded lesions (see Table I). However, the quantities of certain types of damage varied significantly among thiols, particularly the quantity of 3′-phosphoglycolate residues and the partitioning between 5′-phosphate- and nucleoside 5′-aldehyde-ended fragments in SS breaks. The 5′-phosphate-ended DNA, which was always present in both SS and DS breaks at both ACT and AGT, ranged in quantity from <10% with HTP to over 50% with MPA (Table I). The presence of glycolate, on the other hand, was restricted mainly to DS breaks at the T of AGT. MPA produces the highest level of 3′-phosphoglycolate (29%), while DTT and HTP produce little if any glycolate (Table I). The results with HTP are in agreement with the observations by Saito et al. (1989) with NCS-mediated unfractionated damage at a GT step in an oligonucleotide, in which HTP produced 35% C5′ chemistry and 65% C4′ chemistry at T, the latter consisting of <3% glycolate. While HTP produces very few bistranded lesions, DTT produces a significant number, all involving a 4′-hydroxylated abasic site at the T of AGT (Figure 3 and Table I). The relative quantities of 3′-phosphoglycolate produced by the thiols agree well with values determined by Kappen et al. (1991) at GT steps in oligonucleotides. Only very small quantities of 3′-phosphoglycolate were produced by GSH and MPA in SS breaks at ACT (Table I).

A Bias for Bistranded Lesions at AGT. Two lines of evidence point to a predominance of bistranded lesions occuring at AGT and SS breaks at ACT when NCS is activated by GSH. First, densitometric analysis of autoradiograms similar to those shown in Figures 3 and 4 reveals that DS breaks outnumber SS breaks by at least 10:1 at the T of AGT, while SS breaks represent >80% of the damage at ACT. Efficiency of recovery of the duplex SS-damaged and DS-broken DNA does not account for these differences, since virtually all of the DS-broken DNA and >80% of the full length fragments with SS breaks, a small loss taken into account in the calculations, were recovered from the nondenaturing gels. Additionally, SS and DS breaks each have unique relative quantities of breakdown products arising from C4′ and C5′ chemistry, so that the relative contributions of the SS and DS breaks to total (unfractionated) damage at either AGT or ACT can be calculated (data not shown). These calculations are in good agreement with the values derived from densitometry.

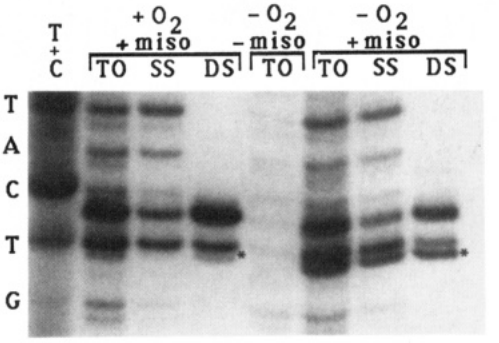

FIGURE 5: Effect of misonidazole on glycolate production at the T of AGT. The 5′-[^{32}P]-labeled *Bam*HI/*Pvu*II fragment was treated with NCS and GSH in the presence of misonidazole under aerobic or anaerobic conditions as described in Materials and Methods, and the hydrazine-treated DNA was resolved on a 60-cm 20% sequencing gel. The first lane is the Maxam–Gilbert C+T chemical sequencing standard; the sequence is defined in the left margin. The designations under each treatment condition signify total unfractionated damage (TO), SS breaks (SS), and DS breaks (DS). Asterisks denote the position of the 3′-phosphoglycolate-ended fragments; the other bands are as in Figure 3, panel A.

Table II: Effect of Misonidazole on NCS-Induced Glycolate Production[a]

	glycolate	phosphate	pyridizine
	$+O_2$, + Misonidazole		
SS	0	47	53
DS	11	19	70
	$-O_2$, + Misonidazole		
SS	28	32	40
DS	37	14	49

[a] The 5′-[^{32}P]-labeled *Bam*HI/*Pvu*II fragment was treated with NCS, GSH, and misonidazole in the presence ($+O_2$) or absence ($-O_2$) of molecular oxygen and subsequently treated with hydrazine as described in Materials and Methods. The values are percentages of AGT cleavage fragments with the following ends: 3′-phosphoglycolate ("glycolate"), 3′-phosphate ("phosphate"), and 3′-phosphopyridizine ("pyridine").

Glycolate Production Increases under Anaerobic Conditions with Misonidazole. When NCS/GSH-mediated DNA damage occurs under anaerobic conditions in the presence of misonidazole, a nitroaromatic radiation sensitizer and oxygen substitute, there is a dramatic increase in the production of 3′-formylphosphate residues in lesions arising at the C5′-position of deoxyribose in DNA (Kappen & Goldberg, 1984; Chin et al., 1987; Kappen et al., 1989). Under similar anaerobic conditions in the presence of misonidazole, Kappen et al. (1991) found an increased ratio of glycolate to pyridizine in unfractionated damage at a GT step in an oligonucleotide. With the working hypothesis that there might be mechanistic similarities in the NCS-mediated damage at the C4′- and C5′-positions, it was decided to examine the partitioning of sugar breakdown products in DS and SS breaks at AGT·ACT when the AP-1 site was treated with NCS in the presence of misonidazole as a substitute for oxygen. The results are shown in an autoradiogram in Figure 5, and the autoradiographic signals are quantitiated in Table II. In control reactions in the presence of both oxygen and misonidazole, the distribution of breakdown products at the T of AGT is similar to the aerobic reaction without misonidazole, in which SS breaks contain no 3′-phosphoglycolate (Table I). These results are in agreement with previous studies of C5′ chemistry and indicate that misonidazole does not compete well with oxygen

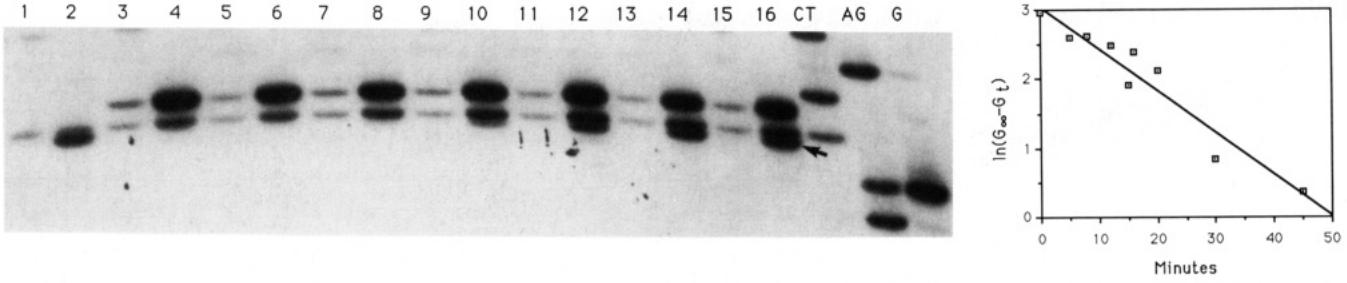

FIGURE 6: Kinetics of NCS-induced 3′-phosphoglycolate production at the T of AGT. (Left) The [^{32}P]-labeled *Bam*HI/*Pvu*II fragment was treated with NCS and GSH, followed at various times by the addition of hydrazine to 100 mM, as described in Materials and Methods. SS and DS breaks were fractionated on a 12% nondenaturing polyacrylamide gel, and the isolated DNA was resolved on a 20% sequencing gel. The times of hydrazine addition are indicated for each pair of lanes as follows: (1 and 2) no hydrazine; (3 and 4) hydrazine and NCS added at the same time; (5–16) hydrazine added 15 s and 1, 5, 15, 45, and 90 min after NCS, respectively. Even-numbered lanes are SS breaks and odd-numbered lanes are DS breaks. The arrow denotes the position of the 3′-phosphoglycolate-ended fragment. (B) A plot of ln ($G_\infty - G_t$) vs time reveals an apparent first-order process with a rate constant of 0.06 min^{-1} ($r^2 = 0.96$) and a $t_{1/2} = 12$ min. G_∞, glycolate as a percentage of total damage at the T of AGT 2 h after NCS was added ($t = \infty$); G_t, percentage glycolate at time = t, the time of hydrazine addition. See text for details.

for the carbon-centered radicals (Kappen & Goldberg, 1984; Chin et al., 1987; Kappen et al., 1989). Under anaerobic conditions, however, misonidazole causes a 3.5-fold increase in the quantity of glycolate-ended residues in bistranded lesions. Strikingly, it results in SS break damage that is nearly one-third 3′-phosphoglycolate. Significant quantities of glycolate were also detected in total DNA damage at the T of AGT when the thiol activator was HTP (data not shown), a thiol not normally producing any detectable glycolate residues (Table I). There was no detectable damage in any experiment when both oxygen and misonidazole were absent (shown in Figure 5 for GSH).

Glycolate Production Is Inhibited by Excess Thiol, Hydrazine, and Borohydride. Two strong reducing agents were found to inhibit the formation of 3′-phosphoglycolate: sodium borohydride and hydrazine, the former causing incomplete inhibition (data not shown). As shown in Figure 6 (left), hydrazine treatment prevents the formation of glycolate without interfering with the formation of 4′-hydroxylation product (as measured by the 3′-phosphopyridizine derivative) or the 3′-phosphate-ended fragments. In fact, there is a reduction in the intensity of the 3′-phosphopyridizine-containing DNA band that parallels the increase in 3′-phosphoglycolate production when hydrazine is added at longer time intervals after NCS treatment (determined by densitometry of lightly exposed autoradiograms). By adding hydrazine at various times after NCS (Figure 6, left), the rate of glycolate formation was determined to be an apparent first-order process with a rate constant of 0.06 min^{-1} (Figure 6, right; $r^2 = 0.96$), which yields a $t_{1/2} = 12$ min. Additionally, increasing concentrations of thiol activator up to 100 mM, GSH in this case, caused a relative reduction in glycolate production, as well (data not shown).

Discussion

Bistranded lesions are probably the most significant damage produced by NCS from the standpoint of cytotoxicity and mutagenicity. *Direct* DS breaks appear to be responsible for the lethality of NCS in cells (Hatayama & Goldberg, 1979) and were found to occur mainly at GT steps, such as AGT·ACT and to a lesser extent TGT·ACT (Dedon & Goldberg, 1990). These GT·AC steps occur commonly in the DNA sequences of several important gene regulatory regions, including the upstream promoter element of the SV40 early promoter, which contains the Sp1 transcription factor binding site; the binding site for AP-1 transcription factors (Fos, Jun, GCN4); and the binding sites for the glucocorticoid receptor and SRF and CREB factors (Mitchell & Tjian, 1983). The same structural features that make this sequence attractive to NCS may also be involved in the protein–DNA interactions that occur at these sites.

In the other known site for NCS-mediated bistranded lesions, AGC·GCT, the formation of an abasic site at the C of AGC correlates with a high rate of G·C to A·T transition mutations in *Escherichia coli* (Povirk & Goldberg, 1985, 1986). These two sites for bistranded lesions would appear to be quite different, but experiments with the model AGT·ACT site demonstrate the close relationship between the bistranded lesions produced by NCS, while at the same time the results reveal critical features of the chemistry of damage at the C4′-position and of the role of the thiol in NCS activity.

The Two Types of Bistranded Lesion Produced by NCS Are Analogous. Biochemical characterization of the lesions occurring at the AP-1 site demonstrates that the AGC·GCT and AGT·ACT sites have many features in common. Both sequences involve a pyrimidine 3′ to the central G, and loss of the exocyclic 2-amino group of the G diminishes cleavage at both sites (Kappen et al., 1988, 1991). Additionally, the next most frequently cleaved sequence analogues for these two sites are TGC and TGT (Povirk & Goldberg, 1986; Dedon & Goldberg, 1990). The bistranded lesions produced at these sites occur with a trinucleotide sequence specificity that gives a 3′-directed 2-bp stagger to the cleavage sites on opposite strands (Povirk et al., 1988; Dedon & Goldberg, 1990). This orientation, along with the 1-bp equivalent of the intercalated naphthoate moiety, places the cleavage sites directly across the minor groove from each other and enables a single molecule of the biradical form of NCS to remove both hydrogen atoms. Modeling and deuterium abstraction studies support a structure with the naphthoate intercalated between the A·T and G·C base pairs and the dehydroindocene structure of activated NCS positioned with the C6 radical near the C5′ hydrogen of the T of GCT and the C2 radical near the C1′-position of the C of AGC (Galat & Goldberg, 1990; Meschwitz & Goldberg, 1991). Similar drug binding at the AGT·ACT site is likely, with the NCS C2 radical nearest the C4′ hydrogen of the T of AGT and the C6 radical near the C5′ hydrogen of the T of ACT. In fact, it has recently been found that deuterium from the C5′ of the T of ACT is abstracted exclusively by C6 of the chromophore (S. M. Meschwitz and I. H. Goldberg, unpublished data). Certain common elements of DNA structure probably contribute to drug binding at both sites: the AG and GC steps in these sequences are associated with significant deflections in the helical axis

of DNA according to the wedge model of DNA curvature (Bolshoy et al., 1991). It has also been noted that the AC·GT dinucleotide step has a very narrow and deep minor groove (Gochin & James, 1990), and it is a likely candidate for the formation of a kink, a conclusion based on the anomalous migration of DNA fragments containing the sequence (Bolshoy et al., 1991).

Similar drug binding at the two sites may explain other common features of the bistranded lesions. First, one strand in both sites is involved more frequently in DS breaks than the other. The abasic site at the C of AGC usually occurs as part of a bistranded lesion, accompanied by a direct break at the T of GCT on the opposite strand (Povirk et al., 1988). However, cleavage at the T of GCT more frequently occurs as SS breaks (Kappen et al., 1989). This is similar to the situation with AGT·ACT, in which lesions at the T of AGT occur predominantly in bistranded lesions and those at the T of ACT mainly as SS breaks. A similar result has been found in self-complementary oligodeoxynucleotides as NCS substrates, where both lesions can be viewed simultaneously on a sequencing gel (S. M. Meschwitz and I. H. Goldberg, unpublished data). It is not apparent yet what features of NCS are responsible for this inequality in cleavage frequency, but differences in reactivity between the two radicals of activated NCS could bias the frequency of cleavage toward a preponderance of SS breaks on one strand relative to the other. Additionally, it is also possible that the C2 radical of NCS is easily quenched by an intramolecular hydrogen abstraction from the α-carbon of the adducted thiol (Chin et al., 1988; Chin & Goldberg, 1992), or that SS and DS lesions are due to different binding orientations, possibly involving different intercalation sites (Galat & Goldberg, 1990).

The bistranded lesion analogy is further strengthened by the presence of an abasic site as the major damage on the strand involved mainly in bistranded lesions: the 2′-deoxyribonolactone of AGC and the 4′-hydroxylated abasic site of AGT. On the strands opposite these abasic sites, the closely opposed lesions at GCT and ACT are direct strand breaks involving mainly C5′ chemistry. Finally, the nature of the thiol appears to affect the quantity of bistranded lesions produced by NCS at both sites in a similar manner, with BME producing fewer abasic sites at AGC and fewer DS breaks at AGT·ACT compared with GSH (Povirk & Goldberg, 1985; Povirk & Houlgrave, 1988; Dedon & Goldberg, 1990). This latter effect will be discussed more fully in the following sections.

There are several differences between the two bistranded lesion sites that may explain their roles in the toxicity of NCS. First, although bistranded lesions at AGT·ACT occur predominantly as indirect breaks due to abasic sites at the T of AGT, there is also a significant component of direct DS breaks (34%; see Table I) that does not appear to occur at AGC·GCT (Povirk & Goldberg, 1985; Povirk & Houlgrave, 1988; Povirk et al., 1988). The latter result is expected since attack at C1′ cannot produce direct breaks. Since DS breaks appear to be responsible for the cytotoxicity of NCS (Hatayama & Goldberg, 1979), these direct DS breaks may correlate better with cytotoxicity than the indirect DS lesions, which require an additional cleavage step with polyamines or with AP endonucleases, to which the NCS-mediated abasic sites are relatively resistant (Povirk & Goldberg, 1985; Povirk & Houlgrave, 1988). The bistranded lesions with abasic sites, on the other hand, appear to be responsible for the mutagenicity associated with NCS (Povirk & Goldberg, 1986). The G·C to A·T transition mutations associated with the abasic site at the C of AGC probably result from the preferential insertion by DNA polymerase of an A opposite the abasic site (Sagher & Strauss, 1983). Such an insertion opposite the abasic site at the T of AGT would be silent, so that mutational activity at AGT·ACT may be relatively low.

The Effects of the Thiol on NCS Hydrogen Atom Selection and Sugar Breakdown Products. The results from the plasmid studies presented in the accompanying paper (Dedon & Goldberg, 1992) and the present work with the AGT·ACT site demonstrate that the nature of the thiol can affect the partitioning of sugar breakdown products and the relative quantities of SS and DS breaks produced by NCS. All the thiols, except HTP, produced bistranded lesions with mainly (>80%) C4′ chemistry at the T of AGT, but there was considerable variation in the quantity of *direct* DS breaks [see Figure 2 of accompanying paper (Dedon & Goldberg, 1992)] and in the partitioning of 4′-hydroxylation product and 3′-phosphoglycolate residues among thiols (Table I and Figure 3A). These two factors are probably related, since there appears to be an association of *direct* DS breaks, produced both in the AGT·ACT model and in plasmids, with 3′-phosphoglycolate residues: thiols that produce abundant glycolate-ended fragments (GSH and MPA) produce the most direct DS breaks, while DTT and HTP produce little glycolate and consequently few direct DS breaks. Small variations in C4′ chemistry partitioning between different AGT·ACT sites in a DNA restriction fragment occur (Z.-W. Jiang and I. H. Goldberg, unpublished observations), which probably accounts for the observation that BME produces fewer direct DS breaks in the plasmid and AGT·ACT models than GSH or MPA yet causes similar partitioning of C4′ chemistry at AGT (Table I).

Part of the effect of the thiol on the partitioning of C4′ chemistry can be explained by the thiol's reducing ability. One measure of the reducing activity of the thiol is the rate at which it undergoes disulfide exchange with oxidized glutathione or Ellman's reagent (Whitesides et al., 1977; Szajewski & Whitesides, 1980). Thiols producing high levels of glycolate and direct DS breaks (e.g., MPA) reduced disulfides more slowly than did thiols producing less glycolate and fewer direct DS breaks (e.g., DTT and HTP). An intermediate rate of disulfide reduction was observed for BME (Whitesides et al., 1977; Szajewski & Whitesides, 1980), as expected from the moderate number of direct DS breaks it produces. Additionally, glycolate production may be related to another reducing activity of thiols: the ability of the thiol to donate a hydrogen atom, which depends on the stability of the thiyl radical generated by hydrogen removal (Hall et al., 1965; Griesbaum, 1970). For example, aromatic thiyl radicals, such as those that occur with HTP, are stabilized by resonance delocalization and are more stable than alkyl thiyl radicals. With DTT, intramolecular hydrogen transfer between vicinal sulfur atoms could serve to stabilize a thiyl radical. Neither of these thiols resulted in the formation of detectable glycolate at AGT·ACT (Table I). Thus, thiols with a high potential for reduction produce less 3′-phosphoglycolate at bistranded lesions, and possibly more 4′-hydroxylation product, than less reducing thiols. This relationship supports the hypothesis, to be discussed later, than NCS-mediated glycolate production, and possibly partitioning of C4′ chemistry in general, involves a reduction-sensitive intermediate, such as an oxyradical species.

HTP clearly behaves differently than thiols such as DTT, which also have high reducing potential. Perhaps for other reasons, HTP-activated drug generates very few, if any, bistranded lesions, even those containing only 4′-hydroxylation

Scheme III: Proposed Mechanisms for the Effect of Misonidazole on NCS-Mediated DNA Damage

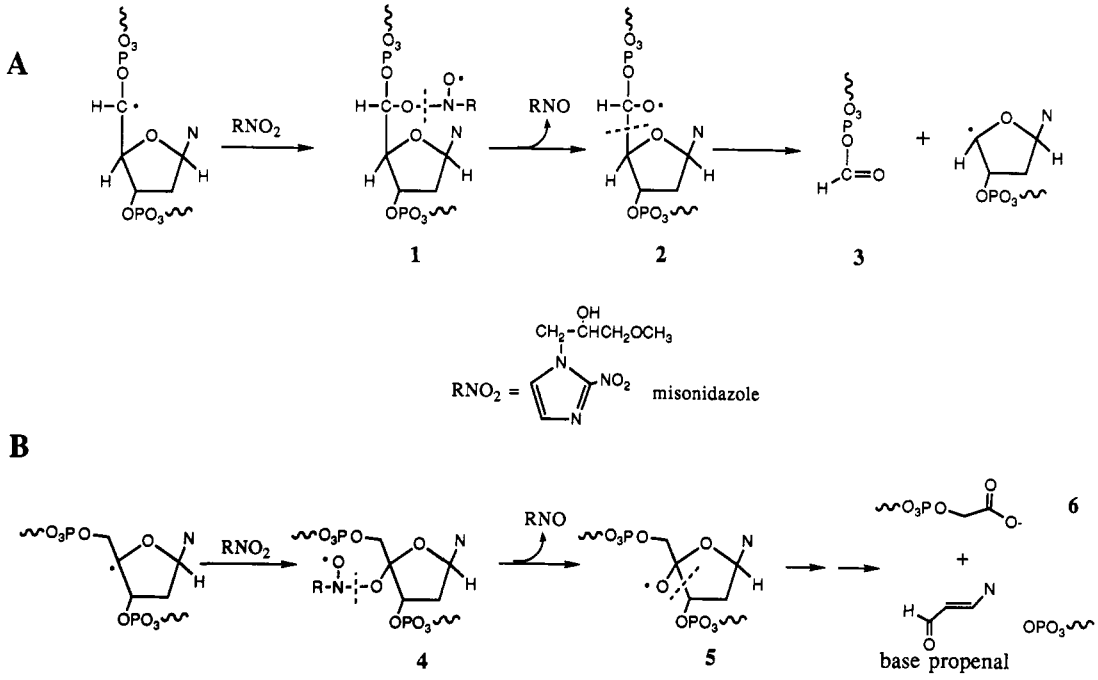

product. It is possible that the aromatic ring stacks with the DNA bases and alters drug orientation. Similar studies with a series of aromatic thiols is an appropriate next step given the unusual behavior of HTP.

While the thiol has significant effects on the rate of activation of NCS, the frequency of bistranded lesions, and the distribution of sugar breakdown products, it does little to determine the selection of the hydrogen atom abstracted by the activated NCS in bistranded lesions: C4′ chemistry predominates at the T of AGT and C5′ chemistry at the T of ACT in bistranded lesions produced by all thiols tested. However, in SS breaks the C4′ cleavage varies from 33% to 84% of the total at the T of AGT and from 24% to 53% at the T of ACT. This suggests that the thiol affects the partitioning between NCS attack sites only in SS breaks, where there are probably less rigorous positioning requirements for abstraction of a single hydrogen atom than for the two hydrogen atoms removed in bistranded lesions. The findings with SS breaks agree with the results obtained by Kappen et al. (1991) at a GT step in an oligonucleotide, in which total DNA damage due to C4′ hydrogen atom abstraction varied between 22% and 42%; SS and DS breaks were not fractionated in these experiments.

The Mechanism of 3′-Phosphoglycolate Formation May Involve an Oxyradical. Unlike bleomycin-induced damage at the C4′ position of deoxyribose (Giloni et al., 1981; Burger et al., 1981; Rabow et al., 1990), there is a strict oxygen requirement for the production of both the glycolate and the abasic site by NCS (Kappen et al., 1991). Abstraction of the C4′ hydrogen atom by activated NCS results in a carbon-centered radical that combines with molecular oxygen to form a peroxyradical (Kappen et al., 1982, 1988, 1991), subsequent reactions of which partition to form either the 4′-hydroxylated abasic site or a strand break with a 3′-phosphoglycolate residue and a 5′-phosphate (von Sonntag, 1980; Saito et al., 1989; Frank et al., 1991) (see Scheme I). The present studies with the AP-1 site reveal several features of the mechanism of formation of 3′-phosphoglycolate.

Under anaerobic conditions, the nitroaromatic radiation sensitizer misonidazole causes an increase in the formation of 3′-phosphoglycolate residues (**6**, Scheme III) in lesions at the T of AGT in both DS and SS breaks, the latter having no detectable glycolate under aerobic conditions (Figure 5). The enhanced production of glycolate raises the possibility that, like the production of 3′-formylphosphate (**3**) following C5′ hydrogen atom abstraction (Kappen & Goldberg, 1984; Chin et al., 1987; Kappen et al., 1989), 3′-phosphoglycolate formation may involve an oxyradical intermediate (**2** and **5**). The mechanistic basis for this possibility lies in the ability of misonidazole to serve as an oxygen substitute in NCS-mediated DNA damage, presumably by forming a labile nitroxyl radical adduct (**1**) with the carbon-centered radical formed when NCS abstracts a hydrogen atom (Chin et al., 1987; Kappen et al., 1989). It appears that subsequent fragmentation results in the formation of an oxyradical at the deoxyribose carbon (**2**) and the nitroso reduction product of misonidazole (Chin et al, 1987; Kappen et al., 1989). At the C5′-position, the fragmentation of the deoxyribose oxyradical produces a labile 3′-formylphosphate moiety (**3**), a 5′-phosphate-ended fragment, a four-carbon sugar residue, and base. This formylphosphate pathway accounts for 10–20% of the damage at the C5′ position under aerobic conditions, with the other 80% consisting of 5′-nucleoside aldehyde (Kappen & Goldberg, 1983). The formylphosphate pathway predominates when misonidazole replaces oxygen. The increase in the production of 3′-phosphoglycolate residues with misonidazole probably occurs by a related mechanism (Scheme IIIB, **4**–**6**). An oxyradical intermediate has also been implicated in the bimolecular decay of the peroxyradical at the C5′ of D-glucose that results in the production of glycolic acid (von Sonntag, 1980).

These findings suggest two mechanistic models for the formation of 3′-phosphoglycolate residues in the presence of dioxygen. In SS lesions, and perhaps in some bistranded lesions, it is possible that the partitioning of C4′ peroxyradical breakdown products begins at the level of the peroxyradical, which can be reduced by thiols and other agents to a hydroxyl group, forming the 4′-hydroxylated abasic site (see the C4′ pathway in Scheme I). Glycolate production in this model depends on the degradation of the peroxyradical to an oxyradical, or possibly on the formation of hydroperoxide by

Scheme IV: Tetraoxide Bridge Model for NCS-Mediated Bistranded Lesions

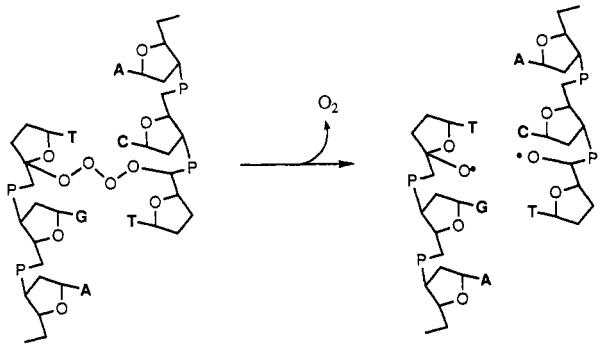

intramolecular hydrogen atom transfer from the C2′-position of deoxyribose, with subsequent breakdown of the sugar residue (Kappen et al., 1991). Both the oxyradical and the hydroperoxide are prone to reduction to a hydroxyl group under reducing conditions. The small quantities of both glycolate and formylphosphate produced in the NCS reactions are consistent with this conclusion. Through the mediation of misonidazole, the quantities of the oxyradical intermediate are apparently increased substantially, raising the probability of the success of the glycolate-forming reactions.

A second model explains the presence of significant quantities of 3′-phosphoglycolate only in bistranded lesions. An intramolecular tetraoxide bridge may form between the peroxyradical at the C5′-position of ACT of one strand and the peroxyradical at the C4′- or C5′-positions of AGT of the other strand, as shown in Scheme IV. A similar proposal, but involving tetraoxide formation between separate strands of polyuridylic acid, has been made to account for chain cleavage due to ionizing radiation (von Sonntag, 1980). Preliminary molecular modeling experiments suggest that the tetraoxide can form between deoxyribose residues staggered 3 bp in a 3′-direction, the equivalent of which occurs in NCS-mediated bistranded lesions, with little alteration of the B-DNA minor-groove dimensions (P. C. Dedon and I. H. Goldberg, unpublished observations). Conditions may be favorable for the tetraoxide cross-linkage since, as discussed earlier, the AGT·ACT site may have an unusual conformation associated with bending or kinking (Bolshoy et al., 1991), and possibly a narrow and deep minor groove (Gochin & James, 1990). Breakdown of the tetraoxide can then occur by several known pathways, including the direct production of two oxyradicals along with molecular oxygen (Scheme IV), as well as by a concerted mechanism that results in glycolate production without an oxyradical intermediate (von Sonntag, 1980; von Sonntag & Schuchmann, 1986). If the bridge were to involve C5′-positions on both strands, this might explain the dominance of the formylphosphate pathway in bistranded lesions at AGT (Table I), where the C5′ chemistry is represented by only 3′- and 5′-phosphate-ended fragments. However, the tetraoxide would have to break down to a species other than an oxyradical at the C5′-position on the other strand or else the oxyradical is rapidly and variably reduced by thiol to a hydroxyl group, since there is no predictable bias in the partitioning of 5′-phosphate- and nucleoside 5′-aldehyde-ended fragments at the T of ACT in bistranded lesions (Table I). The apparent absence of glycolate in SS lesions could result from an inability to form tetraoxides at isolated single lesions, except where misonidazole is included (Figure 5). In essence, misonidazole serves in SS breaks as the second strand of DNA in bistranded lesions bridged by a tetraoxide, with the net result being increased glycolate production.

The relatively slow rate of formation of glycolate ($t_{1/2}$ = 12 min) observed in the hydrazine (and borohydride) time course (Figure 6) suggests that this agent interacts with an intermediate in glycolate formation to prevent its conversion to the final product. Since both hydrazine and sodium borohydride are strong reducing agents, they may be inhibiting glycolate formation at the level of the oxyradical or hydroperoxide, as discussed above, thus converting potential glycolate-forming species into 4′-hydroxylation product. The inhibition of glycolate formation by high levels of thiol is consistent with this interpretation. However, hydrazine and borohydride may also be affecting subsequent steps during the fragmentation of the sugar residue, such as stabilization of a carbonyl group by reduction (borohydride) or Schiff base formation (hydrazine), steps possibly occurring after strand cleavage.

The Mechanisms of Damage Partitioning at C4′ and C5′ May Be Similar. The analysis of the DNA damage at the AGT·ACT site suggests that there are many similarities between the products resulting from the NCS-mediated hydrogen abstraction at the C4′- and C5′-positions. Both lesions involve a partitioning of the peroxyradical to yield either fragmentation of the deoxyribose ring (3′-formylphosphate and 3′-phosphoglycolate pathways) or a lesion in which the main portion of the ring remains intact (4′-hydroxylated abasic site and nucleoside 5′-aldehyde). The latter damage predominates in both cases, while the 3′-phosphoglycolate and 3′-formylphosphate products may both involve an oxyradical intermediate. As in the case of C4′ chemistry, a correlation, albeit a weak one, appears to exist between the reducing power of the thiol and the quantity of 5′-phosphate (presumably arising via the formylphosphate mechanism) at the T of ACT in both DS and SS breaks: less 5′-phosphate is present with BME and DTT in DS breaks than with GSH or MPA (Table I). HTP, the most powerful reducing agent of the thiols, produces very little 5′-phosphate (Table I). Physicochemical differences between C4′ and C5′ oxyradicals, such as accessibility to reducing agents and stability of the oxyradical intermediates, may account for these differences. It is known that carbohydrate peroxyradicals located adjacent to the lactol bridge (C4′ peroxyradicals in the ribose of DNA) are more stable than peroxyradicals at other positions in the sugar (von Sonntag, 1980).

Acknowledgments

We are indebted to Jeanne Thivierge and Wen Shen for their excellent technical assistance and to Lizzy Kappen for her guidance and advice. We thank Michael Greenberg and Victor Rivera, Department of Microbiology and Molecular Genetics, Harvard Medical School, for kindly providing the AP-1 site DNA and Martin Dorf and Carla Martin, Department of Pathology, Harvard Medical School, for the use of the Betascope.

References

Ausubel, F. M., Brent, R., Kingston, R. E., Moore, D. D., Seidman, J. G., Smith, J. A., & Struhl, K. (1989) *Current Protocols in Molecular Biology*, John Wiley and Sons, New York.

Beerman, T., Mueller, G., & Grimmond, H. (1983) *Mol. Pharmacol. 23*, 493–499.

Bolshoy, A., McNamara, P., Harrington, R. E., & Trifonov, E. N. (1991) *Proc. Natl. Acad. Sci. U.S.A. 88*, 2312–2316.

Boye, E., Kohnlein, W., & Skarstad, K. (1984) *Nucleic Acids Res. 12*, 8281–8291.

Burger, R. M., Peisach, J., & Horwitz, S. B. (1981) *J. Biol. Chem. 256*, 11636–11644.
Chin, D.-H., & Goldberg, I. H. (1992) *J. Am. Chem. Soc.* (in press).
Chin, D.-H., Kappen, L. S., & Goldberg, I. H. (1987) *Proc. Natl. Acad. Sci. U.S.A. 84*, 7070–7074.
Dedon, P. C., & Goldberg, I. H. (1990) *J. Biol. Chem. 265*, 14713–14716.
Dedon, P. C., & Goldberg, I. H. (1992) *Biochemistry* (preceding paper in this issue).
Frank, B. L., Worth, L., Jr., Christner, D. F., Kozarich, J. W., Stubbe, J., Kappen, L. S., & Goldberg, I. H. (1991) *J. Am. Chem. Soc. 113*, 2271–2275.
Galat, A., & Goldberg, I. H. (1990) *Nucleic Acids Res. 18*, 2093–2099.
Giloni, L., Takeshita, M., Johnson, F., Iden, C., & Grollman, A. P. (1981) *J. Biol. Chem. 256*, 8608–8615.
Gochin, M., & James, T. L. (1990) *Biochemistry 29*, 11172–11180.
Goldberg, I. H. (1991) *Acc. Chem. Res. 24*, 191–198.
Griesbaum, K. (1970) *Angew. Chem., Int. Ed. Engl. 9*, 273–287.
Hall, D. N., Oswald, A. A., & Greisbaum, K. (1965) *J. Am. Chem. Soc. 30*, 3829–3833.
Hatayama, T., & Goldberg, I. H. (1979) *Biochim. Biophys. Acta 563*, 59–71.
Kappen, L. S., & Goldberg, I. H. (1983) *Biochemistry 22*, 4872–4878.
Kappen, L. S., & Goldberg, I. H. (1984) *Proc. Natl. Acad. Sci. U.S.A. 81*, 3312–3316.
Kappen, L. S., & Goldberg, I. H. (1985) *Nucleic Acids Res. 13*, 1637–1648.
Kappen, L. S., & Goldberg, I. H. (1989) *Biochemistry 28*, 1027–1032.
Kappen, L. S., Goldberg, I. H., & Liesch, J. M. (1982) *Proc. Natl. Acad. Sci. U.S.A. 79*, 744–748.
Kappen, L. S., Chen, C.-Q., & Goldberg, I. H. (1988) *Biochemistry 27*, 4331–4340.
Kappen, L. S., Lee, T. R., Yang, C.-C., & Goldberg, I. H. (1989) *Biochemistry 28*, 4540–4542.
Kappen, L. S., Goldberg, I. H., Wu, S. H., Stubbe, J., Worth, L., & Kozarich, J. W. (1990) *J. Am. Chem. Soc. 112*, 2797–2798.
Kappen, L. S., Goldberg, I. H., Frank, B. L., Worth, L., Christner, D. F., Kozarich, J. W., & Stubbe, J. (1991) *Biochemistry 30*, 2034–2042.
Laskey, R. A., & Mills, A. D. (1975) *Eur. J. Biochem. 56*, 335–341.
Lee, S. H., & Goldberg, I. H. (1989) *Biochemistry 28*, 1019–1026.
Maxam, A., & Gilbert, W. (1980) *Methods Enzymol. 65*, 499–560.
Meschwitz, S. M., & Goldberg, I. H. (1991) *Proc. Natl. Acad. Sci. U.S.A. 88*, 3047–3051.
Mitchell, P. J., & Tjian, R. (1983) *Science 245*, 371–378.
Poon, R., Beerman, T. A., & Goldberg, I. H. (1977) *Biochemistry 16*, 486–493.
Povirk, L. F., & Goldberg, I. H. (1985) *Proc. Natl. Acad. Sci. U.S.A. 82*, 3182–3186.
Povirk, L. F., & Goldberg, I. H. (1986) *Nucleic Acids Res. 14*, 1417–1426.
Povirk, L. F., & Houlgrave, C. W. (1988) *Biochemistry 27*, 3850–3857.
Povirk, L. F., Houlgrave, C. W., & Han, Y.-H. (1988) *J. Biol. Chem. 263*, 19263–19266.
Rabow, L., Stubbe, J., Kozarich, J. W., & Gerlt, J. A. (1986) *J. Am. Chem. Soc. 108*, 7130.
Rabow, L. E., Stubbe, J., & Kozarich, J. W. (1990) *J. Am. Chem. Soc. 112*, 3196–3203.
Sagher, D., & Strauss, B. (1983) *Biochemistry 22*, 4518–4526.
Saito, I., Kawabata, H., Fujiwara, T., Sugiyama, H., & Matsuura, T. (1989) *J. Am. Chem. Soc. 111*, 8302–8303.
Sugiyama, H., Xu, C., Murugesan, N., Hecht, S. M., van der Marel, G. A., & van Boom, J. H. (1988) *Biochemistry 27*, 58–67.
Szajewski, R. P., & Whitesides, G. M. (1980) *J. Am. Chem. Soc. 102*, 2011–2026.
Takeshita, M., Kappen, L. S., Grollman, A. P., Eisenberg, M., & Goldberg, I. H. (1981) *Biochemistry 20*, 7599–7506.
von Sonntag, C. (1980) *Adv. Carbohydr. Chem. Biochem. 37*, 7–77.
von Sonntag, C., & Schuchmann, H.-P. (1986) *Int. J. Radiat. Biol. 49*, 1–34.
Whitesides, G. M., Lilburn, J. E., & Szajewski, R. P. (1977) *J. Org. Chem. 42*, 332–338.